# Proton conduction in two Cu/Zn dimer-based hydrogen-bonded supramolecular frameworks from imidazole multi-carboxylate

Qingxu Wang,[a] Zhejun Ye,[a] Guoqing Shi,[b] Kaimeng Guo,[a] and Gang Li*[a]

[a] *College of Chemistry and Green Catalysis Center, Zhengzhou University, Zhengzhou 450001, Henan, China*

[b] *School of Food and Bioengineering, Zhengzhou University of Light Industry, Zhengzhou 450052, Henan, China*

**e-mail: gangli@zzu.edu.cn*

## Supporting information

**Table S1.** Selected bond distances (Å) and angles (deg) for compounds **1** and **2**

| | | | |
|---|---|---|---|
| Complex **1** | | | |
| Cu(1)-N(2)#1 | 2.192(2) | Cu(1)-N(3) | 1.985(2) |
| Cu(1)-N(4) | 2.019(2) | Cu(1)-O(5)#1 | 1.971(2) |
| Cu(1)-O(6) | 2.008(2) | | |
| N(3)-Cu(1)-N(4) | 82.49(10) | N(3)-Cu(1)-O(6) | 93.83(10) |
| N(4)-Cu(1)-N(2) #1 | 124.92(9) | O(5)#1-Cu(1)-N(2)#1 | 80.71(9) |
| O(5)#1-Cu(1)-N(3) | 175.06(10) | O(5)#1-Cu(1)-N(4) | 93.35(10) |
| O(5)#1-Cu(1)-O(6) | 91.11(10) | N(3)-Cu(1)-N(2)#1 | 99.46(9) |
| Complex **2** | | | |
| N(3)-Zn(1) | 2.139(3) | O(5)-Zn(1) | 1.973(2) |
| Zn(1)-N(2)#1 | 2.067(2) | N(4)-Zn(1) | 2.080(3) |
| Zn(1)-O(4)#1 | 2.097(3) | | |
| O(5)-Zn(1)-N(2)#1 | 103.80(9) | O(5)-Zn(1)-N(3) | 93.86(11) |
| O(5)-Zn(1)-N(4) | 139.86(10) | O(5)-Zn(1)-O(4)#1 | 95.40(11) |
| N(2)#1-Zn(1)-N(3) | 99.33(11) | N(2)#1-Zn(1)-N(4) | 116.26(10) |
| N(2)#1-Zn(1)-O(4)#1 | 80.62(10) | O(4)#1-Zn(1)-N(3) | 170.47(10) |

Symmetry transformations used to generate equivalent atoms for **1**：#1: 2-X, 2-Y, 2-Z; For **2**: #1: 1-X, +Y, 1/2-Z.

**Table S2.** Hydrogen bonding parameters for **1** and **2**

| D-H...A | d(D-H) | d(H...A) | d(D...A) | ∠(DHA) |
|---|---|---|---|---|
| **1** | | | | |
| O(2)-H(2)...O(3) | 0.937(19) | 1.56(2) | 2.494(4) | 172(5) |
| O(7)-H(7A)...O(5)#1 | 1.02(8) | 2.29(7) | 3.003(13) | 126(7) |
| N(1)-H(1)...O(4) | 0.90 | 2.74 | 3.422(19) | 132.6 |
| N(1)-H(1)...O(8)#2 | 0.90 | 2.03 | 2.753(6) | 135.8 |
| O(8)-H(8A)...O(4)#3 | 0.85 | 2.27 | 2.923(19) | 134.2 |
| O(8)-H(8B)...O(4)#4 | 0.85 | 2.13 | 2.79(2) | 134.3 |
| O(8)-H(8B)...O(8)#5 | 0.85 | 2.54 | 3.297(14) | 148.8 |

| | | | | |
|---|---|---|---|---|
| O(8A)-H(8AA)...O(5)#1 | 0.85 | 2.74 | 3.309(8) | 126.0 |
| O(8A)-H(8AA)...O(7)#3 | 0.85 | 2.32 | 3.132(19) | 161.0 |
| O(8A)-H(8AA)...O(7) | 0.85 | 2.23 | 3.018(18) | 153.4 |
| **2** | | | | |
| N(1)-H(1)...O(6)#1 | 0.86 | 1.95 | 2.766(3) | 157.6 |
| O(2)-H(2)...O(3) | 0.82 | 1.70 | 2.522(4) | 178.1 |

Symmetry transformations used to generate equivalent atoms for **1**：#1: 2-X, 2-Y, 2-Z; #2: 1+X, +Y, +Z; #3: 1-X, 2-Y, 1-Z; #4: -1+X, +Y, +Z; #5: -X, 2-Y, 1-Z. For **2**: #1: 1-X, -Y, 1-Z.

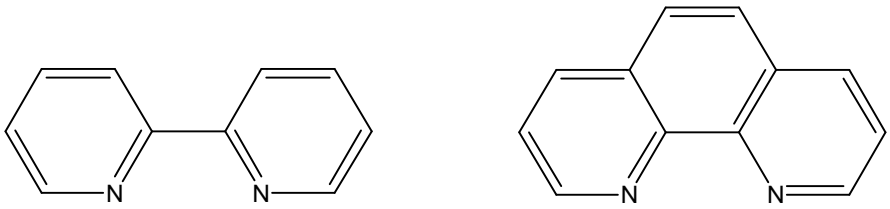


(a) (b)

**Scheme S1.** The chemical structure of 2,2'-bipy and phen.

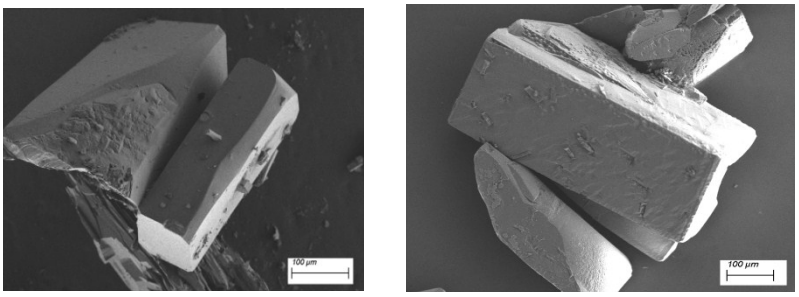


(a) (b)

(b)

**Fig. S1** SEM pictures of HSFs **1**(a) and **2**(b).

For complexes **1** and **2**, the impedance plots give a single semicircle at high frequency and a spur at low frequency. Equivalent circuits LR(C(R(Q(R(C(RW)))))) and LR(CR(QR)(RW)) can well fit the measured the impedance plots of **1** and **2**, respectively. The representative fits are shown in Figs. S2 and S3.

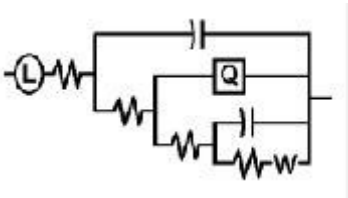


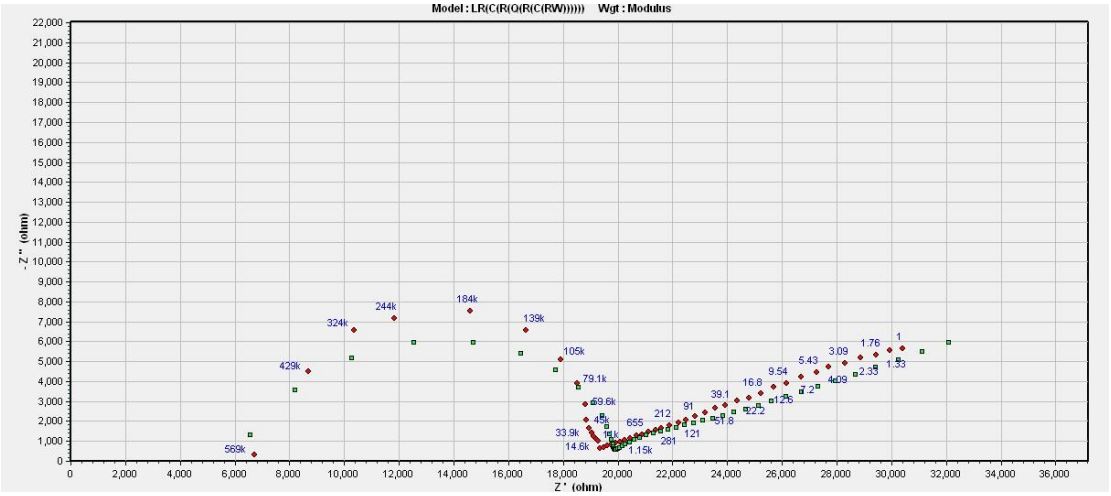


(a)

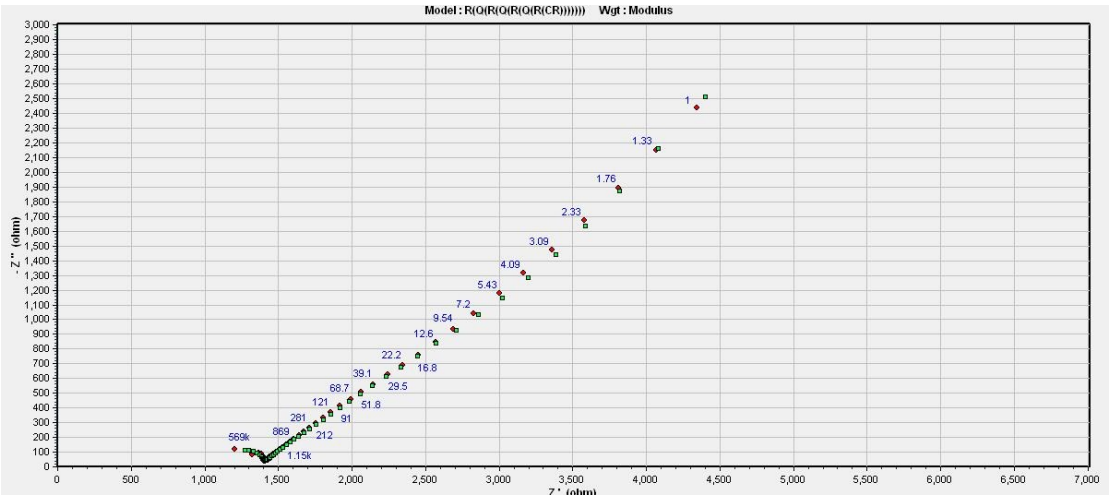


(b)

**Fig. S2** Nyquist plots for a polycrystalline sample of **1** under 30°C (a) and 100°C (b) at 98% RH. Red circle and green square are the measured impedance spectroscopy values and the fits of the impedance data to the equivalent circuit of LR(C(R(Q(R(C(RW)))))).

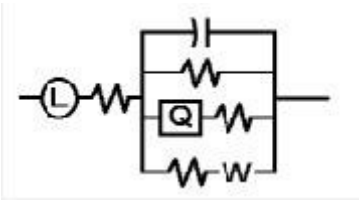


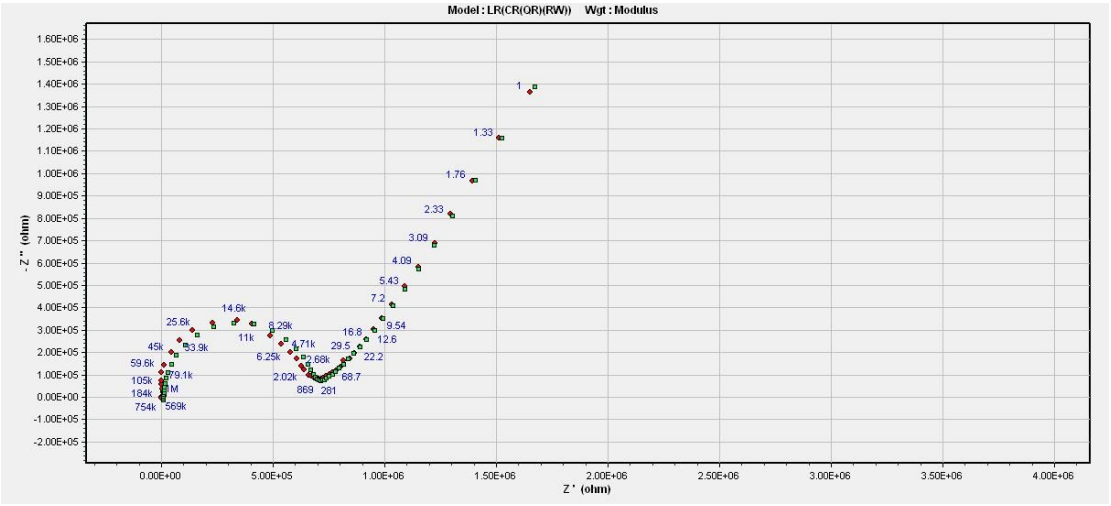


(a)

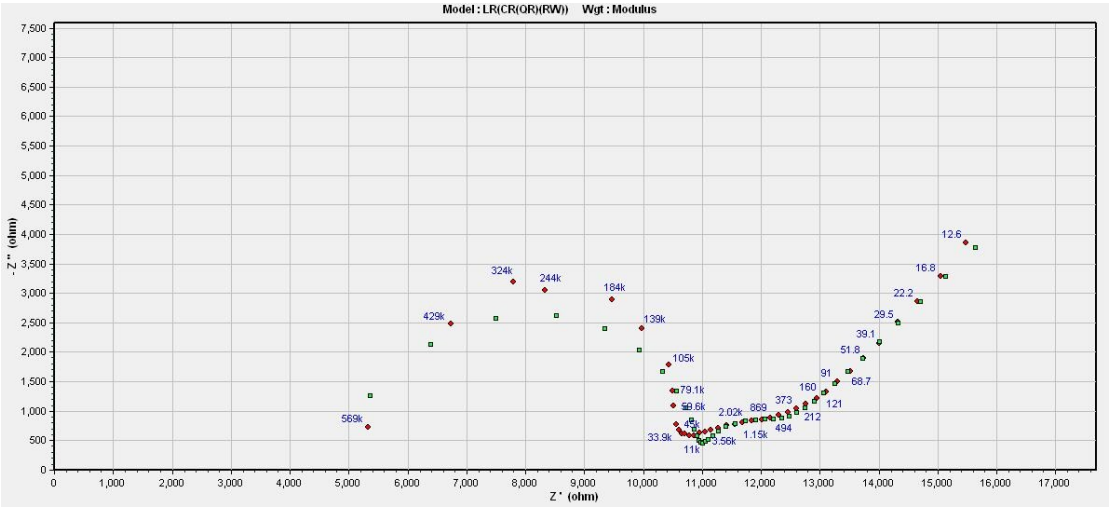


(b)

**Fig. S3** Nyquist plots for a polycrystalline sample of **2** under 30°C (a) and 100°C (b) at 98% RH. Red circle and green square are the measured impedance spectroscopy values and the fits of the impedance data to the equivalent circuit of LR(CR(QR)(RW)).

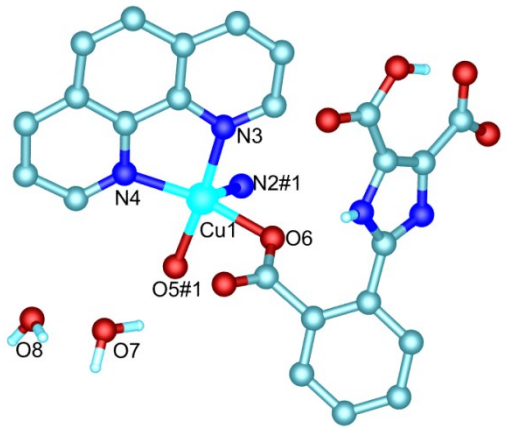


**Fig. S4** Molecular structure of complex **1**.

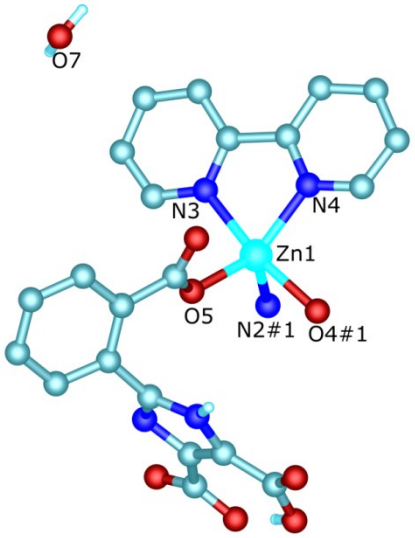


**Fig. S5** Molecular structure of complex **2**.

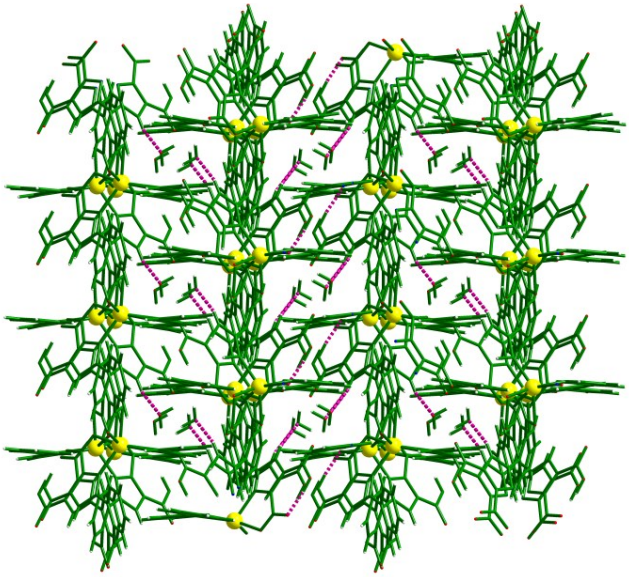

**Fig. S6** Molecular packing of complex **2**.

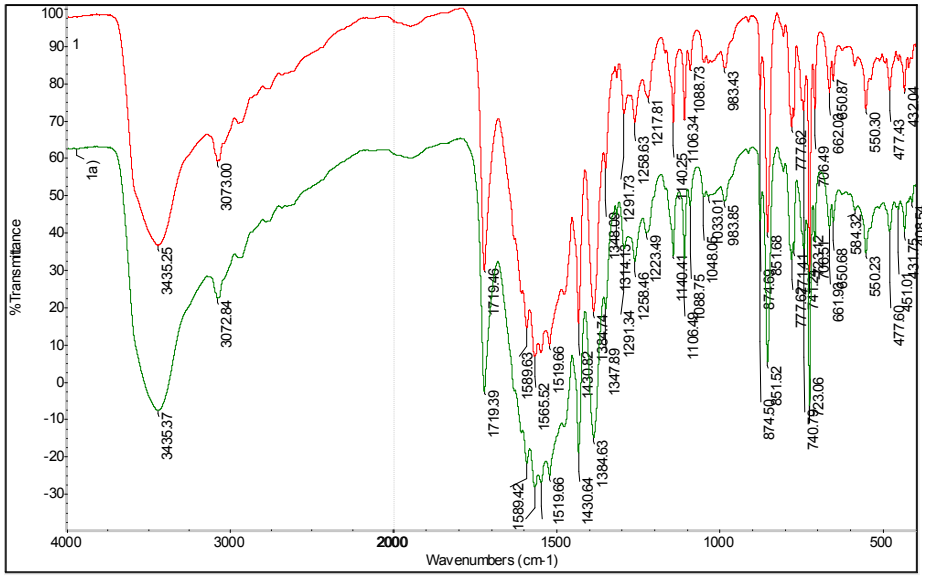


**Fig. S7** The IR spectra of **1** (red line) and the "activated" sample of **1** (green line).

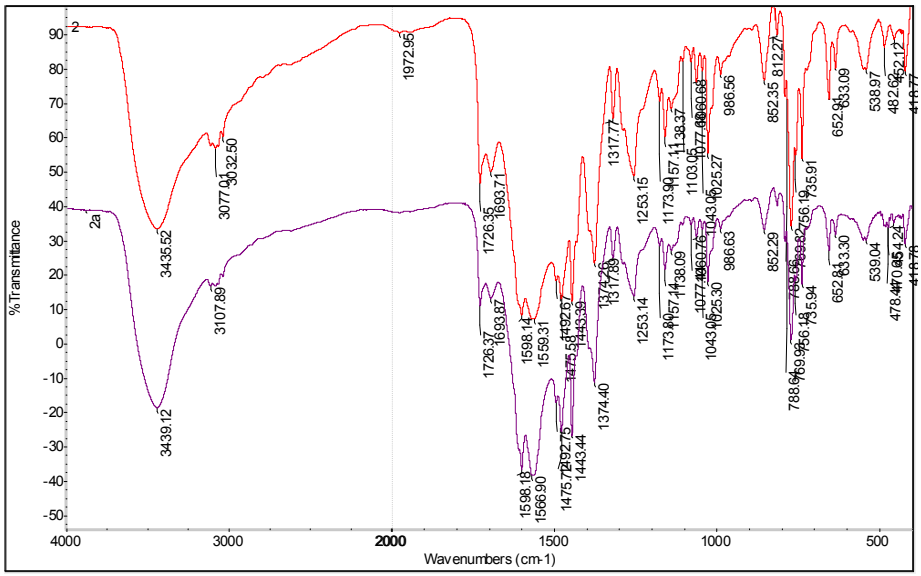


**Fig. S8** The IR spectra of **2** (red line) and the "activated" sample of **2** (purple line).

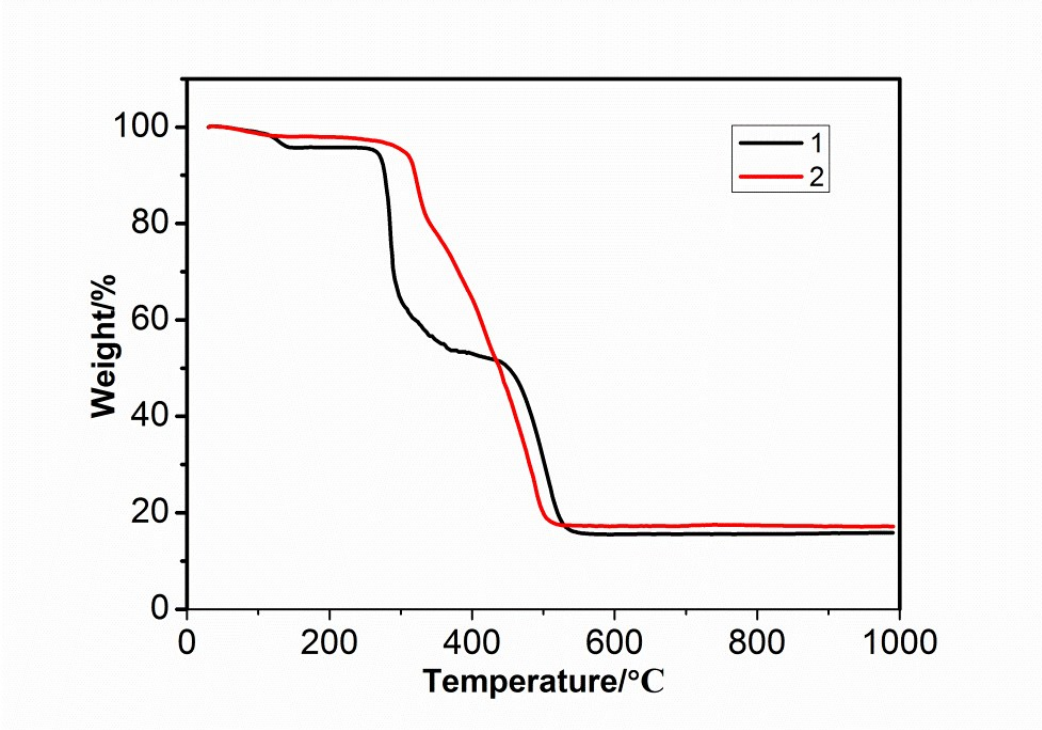


**Fig. S9** TG analysis profiles of complexes **1**and **2**.

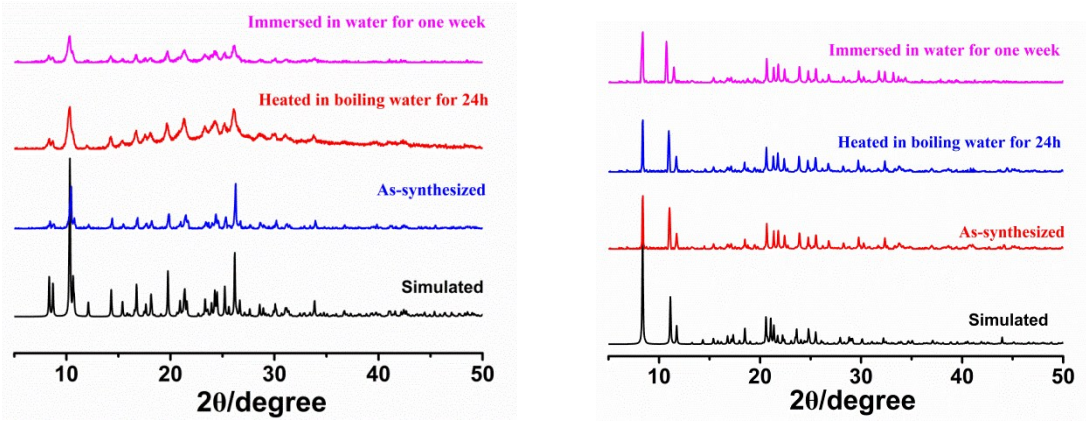


(a) (b)

**Fig. S10** PXRD patterns of **1** (a) and **2** (b): The simulated ones from the single-crystal data, as-synthesized, and after water-treatment samples.

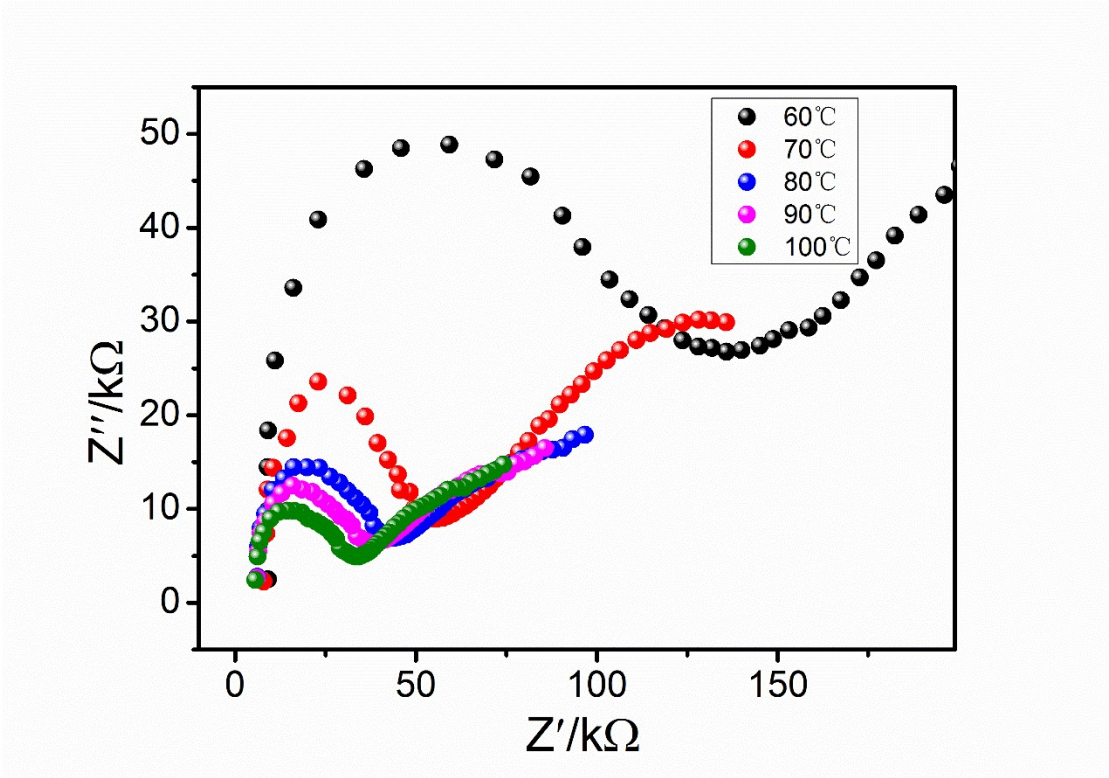


**Fig. S11** AC impedance spectra of complex **1** in the range of 60-100 °C at 75% RH.

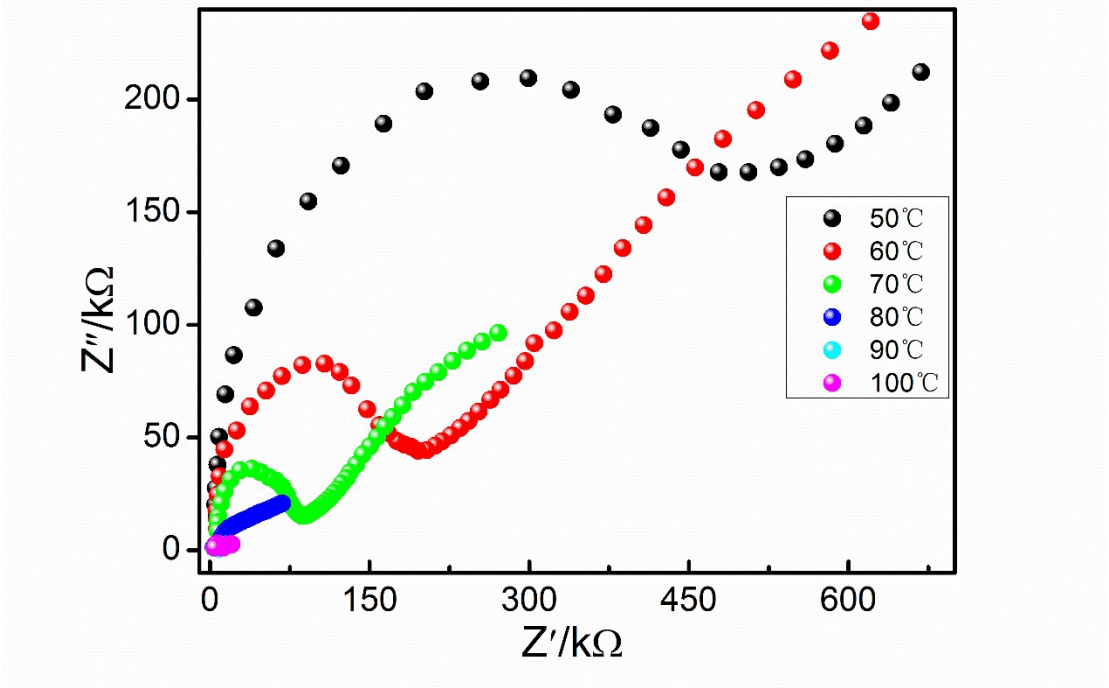


**Fig. S12** AC impedance spectra of complex **1** in the range of 50-100 °C at 85% RH.

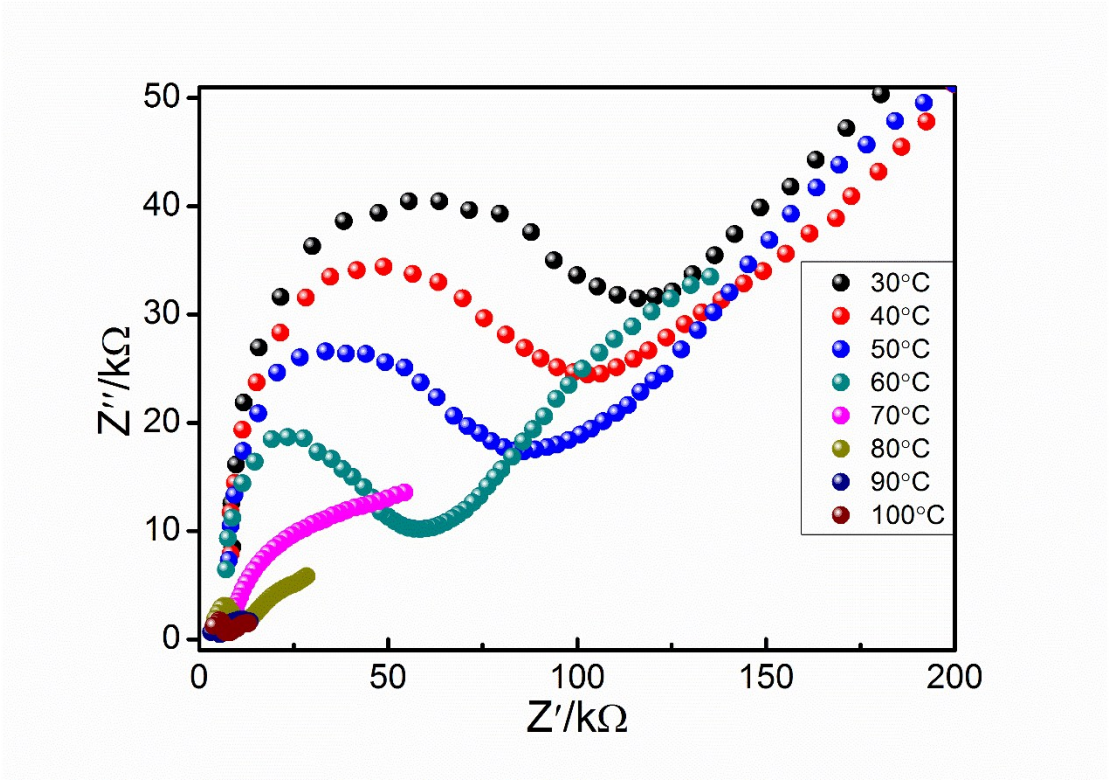


**Fig. S13** AC impedance spectra of complex **1** in the range of 30-100 °C at 93%RH.

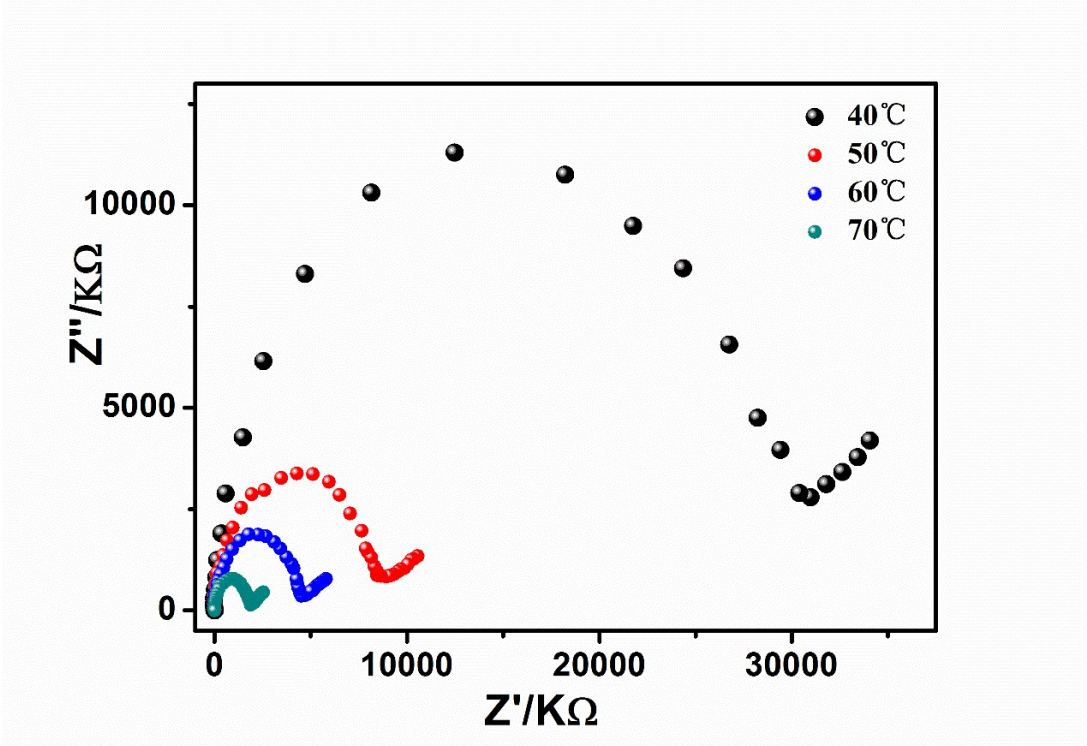

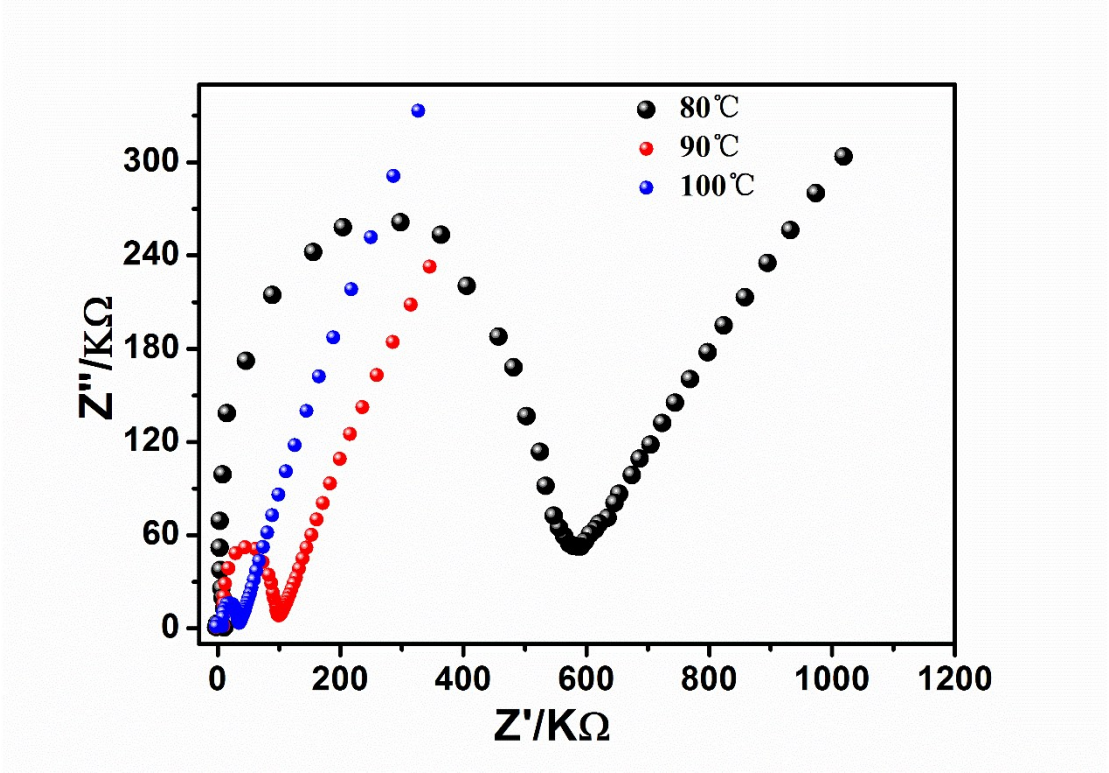


**Fig. S14** AC impedance spectra of complex **2** in the range of 40-100 °C at 75% RH.

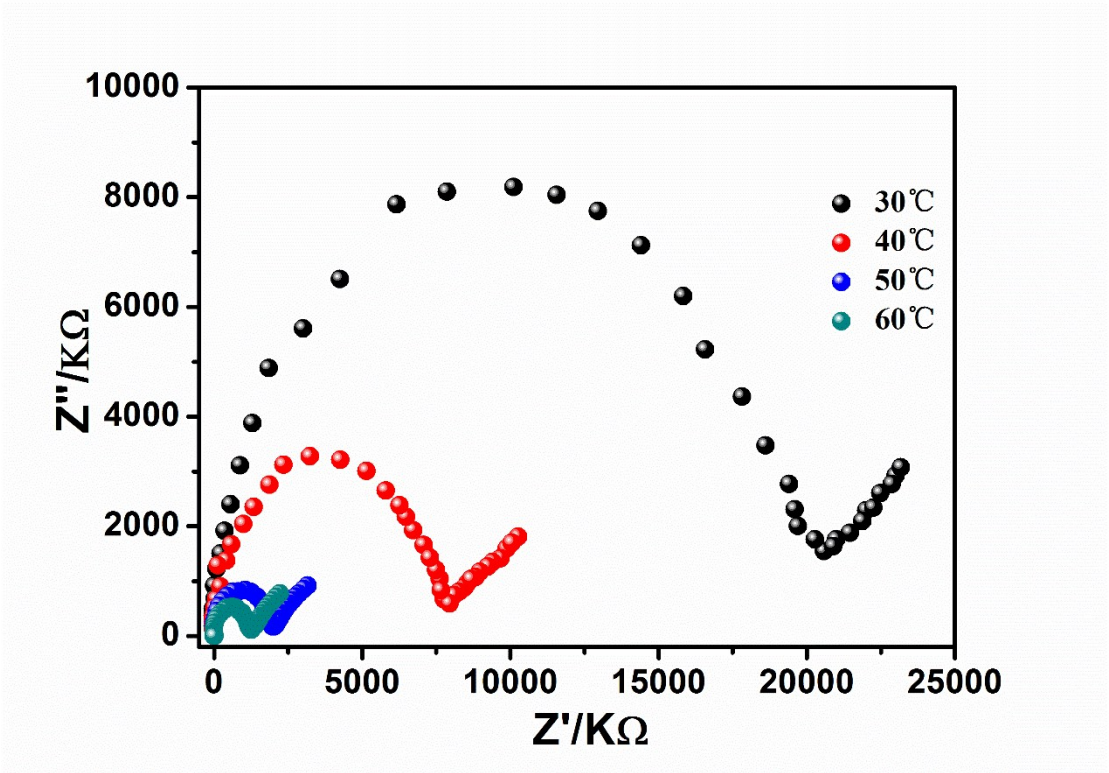

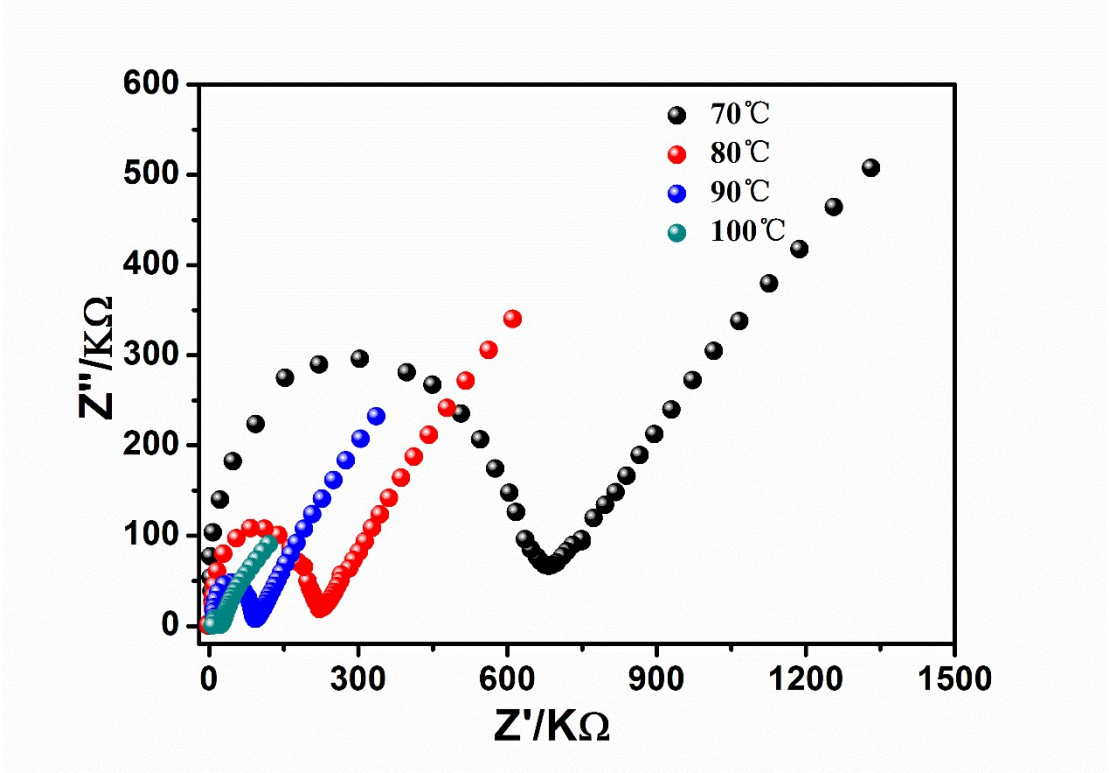


**Fig. S15** AC impedance spectra of complex **2** in the range of 30-100 °C at 85% RH.

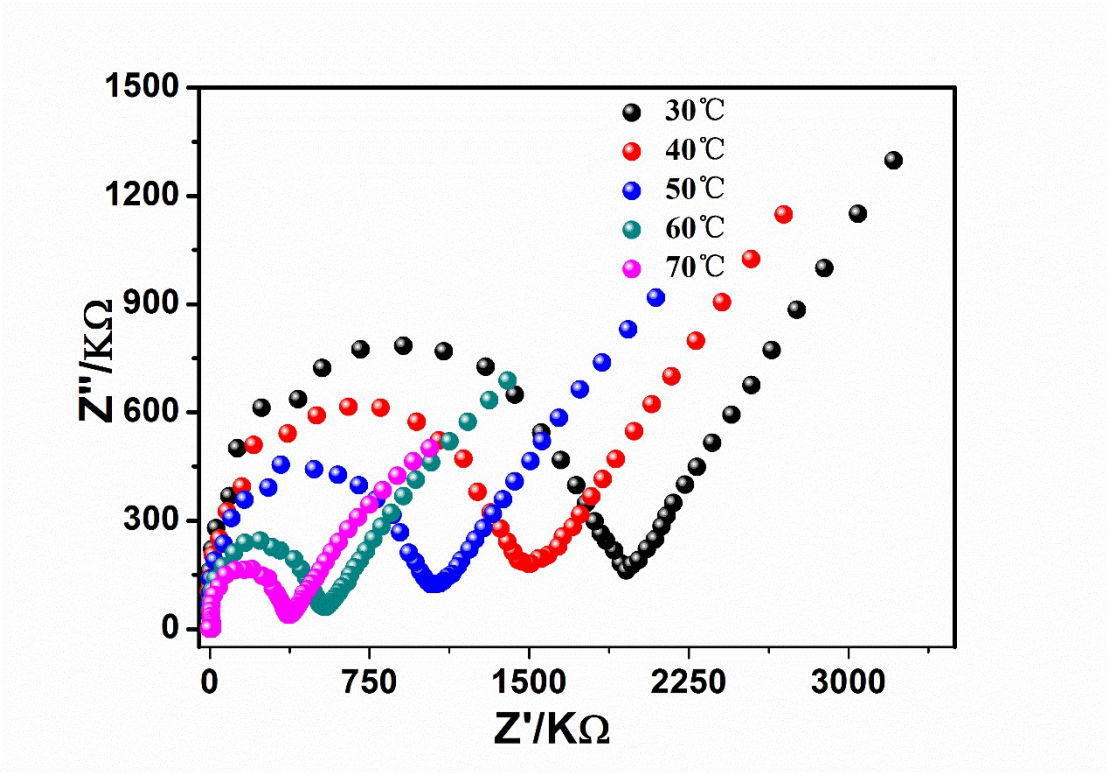

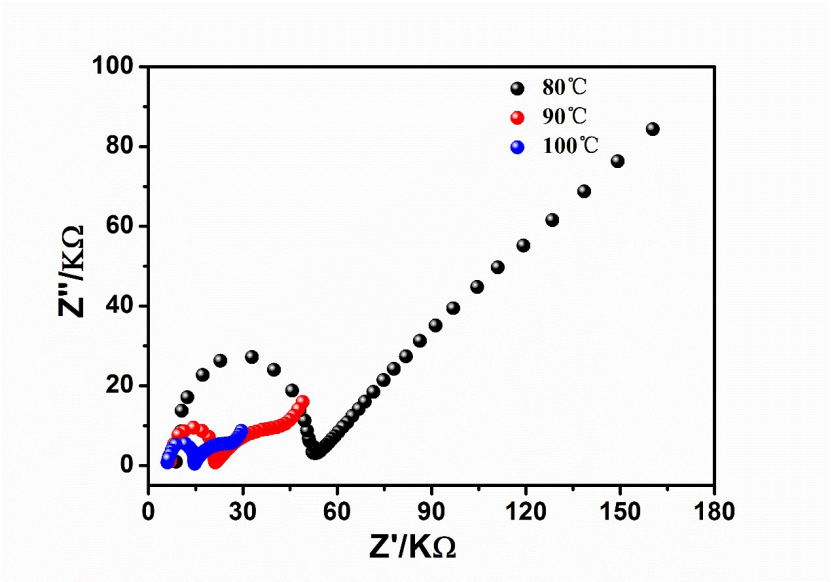


**Fig. S16** AC impedance spectra of complex **2** in the range of 30-100 °C at 93% RH.

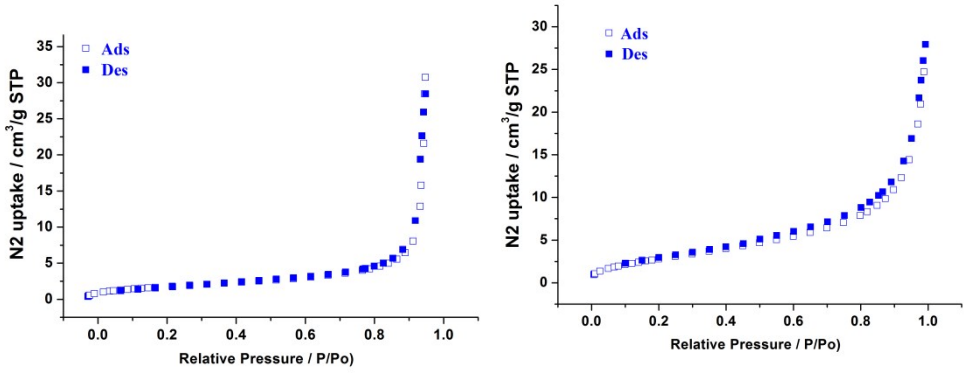


(a) (b)

**Fig. S17** $N_2$ adsorption and desorption isotherms at -196 °C for dimers **1**(a) and **2** (b).

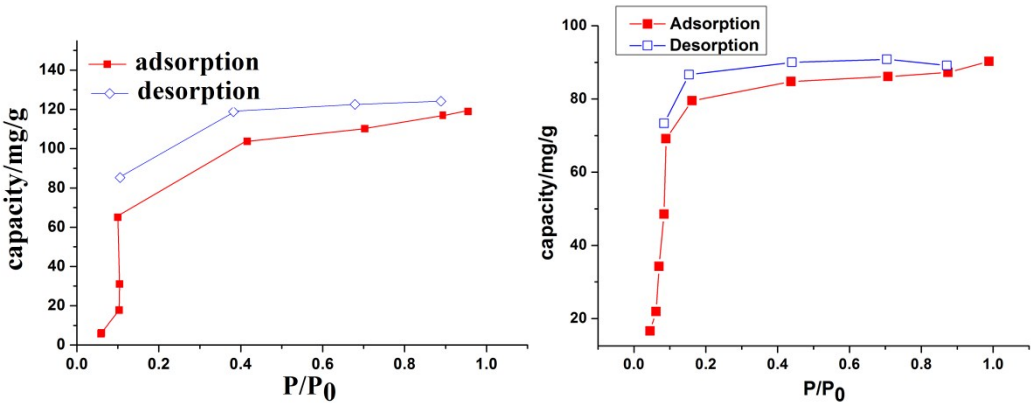


(a) (b)

**Fig. S18** Water vapor adsorption/desorption isotherms of **1**(a) and **2**(b) at 25 °C.

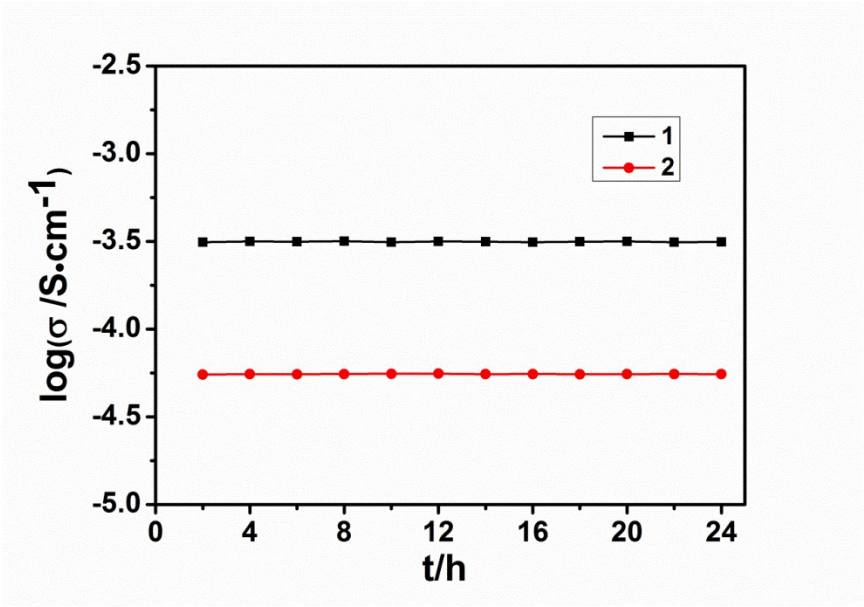


**Fig. 19** Time-dependent conductivity of dimers **1** and **2** under 100 °C and 98% RH.